ELSEVIER

www.elsevier.nl/locate/jorganchem

Journal of Organometallic Chemistry 588 (1999) 211–221

Journal of Organo metallic Chemistry

Syntheses, reactivities and crystal structures of triosmium clusters with imidazo(1,2-*a*)pyridine ligand

Jasmeen Akther [a], Kazi A. Azam [a], Anjoli R. Das [a], Michael B. Hursthouse [b,1], Shariff E. Kabir [c], K.M. Abdul Malik [b,*], Edward Rosenberg [d], Markus Tesmer [c], Heinrich Vahrenkamp [c]

[a] *Department of Chemistry, Jahangirnagar University, Savar, Dhaka 1342, Bangladesh*
[b] *Department of Chemistry, Cardiff University, PO Box 912, Park Place, Cardiff CF1 3TB, UK*
[c] *Institut für Anorganische und Analytische Chemie, Universität Freiburg, Albertstrasse 21, D-79104 Freiburg, Germany*
[d] *Department of Chemistry, The University of Montana, Missoula, MT 59812, USA*

Received 4 May 1999; received in revised form 23 June 1999

Abstract

Treatment of the lightly stabilized cluster $[\mathrm{Os_3(CO)_{10}(MeCN)_2}]$ with excess imidazo(1,2-*a*)pyridine at 25°C yields $[(\mu\text{-H})\mathrm{Os_3(CO)_{10}}(\mu\text{-}1,2\text{-}\eta^2\text{-}\mathrm{C_7H_5N_2})]$ (**7**) and $[(\mu\text{-H})\mathrm{Os_3(CO)_{10}}(\mu\text{-}1,7\text{-}\eta^2\text{-}\mathrm{C_7H_5N_2})]$ (**8**) in 30 and 40% yields, respectively. The structures of **7** and **8** reveal that in the former the heterocyclic ligand is coordinated via the imino nitrogen and C(2) carbon atoms, whereas in the latter the ligand is coordinated via the imino nitrogen and C(7) carbon atoms. The reaction of $[\mathrm{Os_3(CO)_{11}(MeCN)}]$ with excess imidazo(1,2-*a*)pyridine at 25°C gives the N-coordinated imidazo(1,2-*a*)pyridine compound $[\mathrm{Os_3(CO)_{11}}(\eta^1\text{-}\mathrm{C_7H_6N_2})]$ (**9**), which on refluxing in octane undergoes both C(2)–H and C(7)–H bond activation, producing **7** and **8** in 32 and 15% yields, respectively. Compound **9** is similar to $[\mathrm{Os_3(CO)_{11}(MeCN)}]$ in that its N-coordinated ligand is labile and can easily be replaced by various two-electron donors L yielding $[\mathrm{Os_3(CO)_{11}(L)}]$ {L = $\mathrm{PPh_3}$; $\mathrm{P(OMe)_3}$ or ^{t}BuNC}. Compounds **7** and **8** further react with imidazo(1,2-*a*)pyridine to afford $[(\mu\text{-H})_2\mathrm{Os_3(CO)_8}(\mu\text{-}1,2\text{-}\eta^2\text{-}\mathrm{C_7H_5N_2})_2]$ (**10**) and $[(\mu\text{-H})_2\mathrm{Os_3(CO)_8}(\mu\text{-}1,7\text{-}\eta^2\text{-}\mathrm{C_7H_5N_2})(\mu\text{-}1,2\text{-}\eta^2\text{-}\mathrm{C_7H_5N_2}]$ (**11**), respectively. Compound **11** contains two imidazo(1,2-*a*)pyridine-derived ligands formed by activation of C(2)–H and C(7)–H bonds, whereas both the heterocyclic ligands in **10** are formed by activation of C(2)–H bonds. Both compounds **7** and **8** react with $\mathrm{PPh_3}$ at 110°C to yield the monosubstituted products $[(\mu\text{-H})\mathrm{Os_3(CO)_9}(\mu\text{-}1,2\text{-}\eta^2\text{-}\mathrm{C_7H_5N_2})(\mathrm{PPh_3})]$ (**12**) and $[(\mu\text{-H})\mathrm{Os_3(CO)_9}(\mu\text{-}1,7\text{-}\eta^2\text{-}\mathrm{C_7H_5N_2})(\mathrm{PPh_3})]$ (**13**). The structures of **7**, **8**, **9** and **11** have been established by X-ray crystallography.

Keywords: Triosmium; Imidazo(1,2-*a*)pyridine; Carbonyl; Hydride; Crystal structure

---

1. Introduction

Intramolecular activation of C–H, N–H and C–N bonds of nitrogen-containing aromatic heterocycles by transition metals has been widely investigated [1–20], yet there is still considerable interest in such studies because of the relevance of the complexes obtained in understanding the catalytically important hydrodenitrogenation (HDN) process. We have recently reported the ambient temperature reactions of dinitrogen heterocycles such as imidazoles and pyrazoles [21] and nitrogen- and sulfur-containing heterocycles such as thiazole [22,23] and 4-methylthiazole [24] with $[\mathrm{Ru_3(CO)_{12}}]$ and the lightly stabilized cluster $[\mathrm{Os_3(CO)_{10}(MeCN)_2}]$. However, there are very few studies of the interaction of trimetallic clusters of osmium and ruthenium with polynuclear heteroaromatic nitrogen heterocycles. The direct reactions of $[\mathrm{M_3(CO)_{12}}]$ (M = Os, Ru) with quinolines have previously been examined at elevated temperatures and gave mono- and bis(quinoline) complexes $[(\mu\text{-H})\mathrm{M_3(CO)_{10}}(\mu\text{-}1,2\text{-}\eta^2\text{-}\mathrm{C_9H_6N})]$ (**1**, M = Os; **2**, M = Ru) and $[(\mu\text{-H})_2\mathrm{M_3(CO)_8}(\mu\text{-}\eta^2\text{-}\mathrm{C_9H_6N})_2]$ (**3**, M = Os; **4**, M = Ru) (Scheme 1) in which the C(2) car-

---

* Corresponding author. Tel.: + 44-1222-874950; fax: + 44-1222-874030.

E-mail address: malikka@cardiff.ac.uk (K.M. Abdul Malik)

[1] Present address: Department of Chemistry, University of Southampton, Highfield, Southampton SO17 1BJ, UK.

0022-328X/99/$ - see front matter © 1999 Elsevier Science S.A. All rights reserved.
PII: S0022-328X(99)00377-0

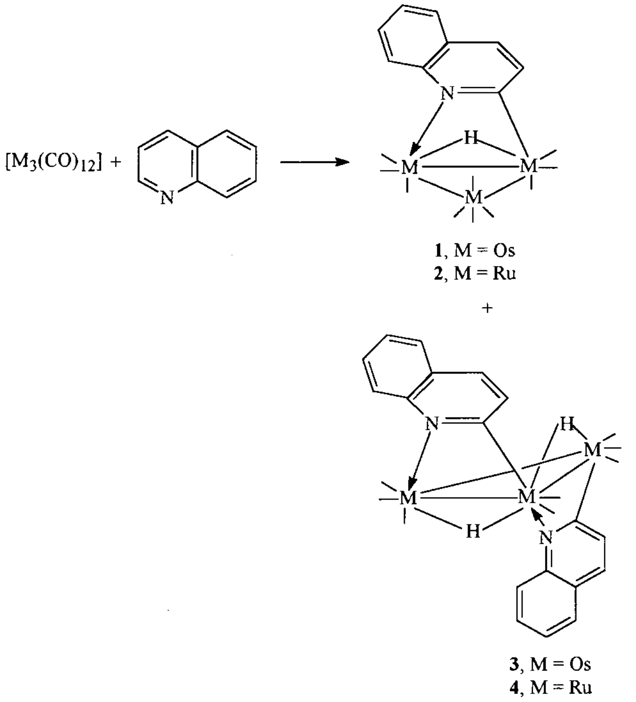

Scheme 1.

bon–hydrogen bond of the quinoline ring has been oxidatively added to the cluster [1,2].

It was reported recently [25] that the ambient temperature reaction of quinoline with $[Os_3(CO)_{10}(MeCN)_2]$ yields the compound $[(\mu\text{-H})Os_3(CO)_{10}(\mu\text{-}1,8\text{-}\eta^2\text{-}C_9H_6N)]$ (**5**) as the major product, in which the C(8) carbon–hydrogen bond has been oxidatively added to the cluster, along with a small amount of the known compound **1** [1]. Compound **5** was decarbonylated to give the highly reactive $46e^-$ cluster $[(\mu\text{-H})Os_3(CO)_9(\mu_3\text{-}1,8\text{-}\eta^2\text{-}C_9H_6N)]$ (**6**) (Scheme 2), in which the quinoline ring is bound to the trimetallic core by a three-center–one-electron bond with the C(8) carbon bridging two metal atoms along with coordination of the nitrogen lone pair to the third osmium [25].

As a part of our on-going work in the field, we investigated the reactions of imidazo(1,2-*a*)pyridine with the lightly stabilized cluster $[Os_3(CO)_{10}(MeCN)_2]$. It was expected that such a cluster would favor oxidative addition of the C(7)–H bond of imidazo-(1,2-*a*)pyridine resulting in the formation of $[(\mu\text{-H})Os_3(CO)_{10}(\mu\text{-}1,7\text{-}\eta^2\text{-}C_7H_5N_2)]$ which, in turn, would give the $46e^-$ cluster $[(\mu\text{-H})Os_3(CO)_9(\mu_3\text{-}1,7\text{-}\eta^2\text{-}C_7H_5N_2)]$ as it does for quinoline and substituted quinolines. We also investigated the reactions of $[Os_3(CO)_{11}(MeCN)]$ with imidazo(1,2-*a*)pyridine to gain an insight into the initial mode of bonding of the N-heterocycle and its subsequent conversion to the C–H-activated products. The results of these studies are presented herein.

2. Results and discussion

Treatment of the lightly stabilized cluster $[Os_3(CO)_{10}(MeCN)_2]$ with imidazo(1,2-*a*)pyridine at ambient temperature afforded two major compounds $[(\mu\text{-H})Os_3(CO)_{10}(\mu\text{-}1,2\text{-}\eta^2\text{-}C_7H_5N_2)]$ (**7**) and $[(\mu\text{-H})Os_3(CO)_{10}(\mu\text{-}1,7\text{-}\eta^2\text{-}C_7H_5N_2)]$ (**8**) in 30 and 40% yields, respectively (Scheme 3).

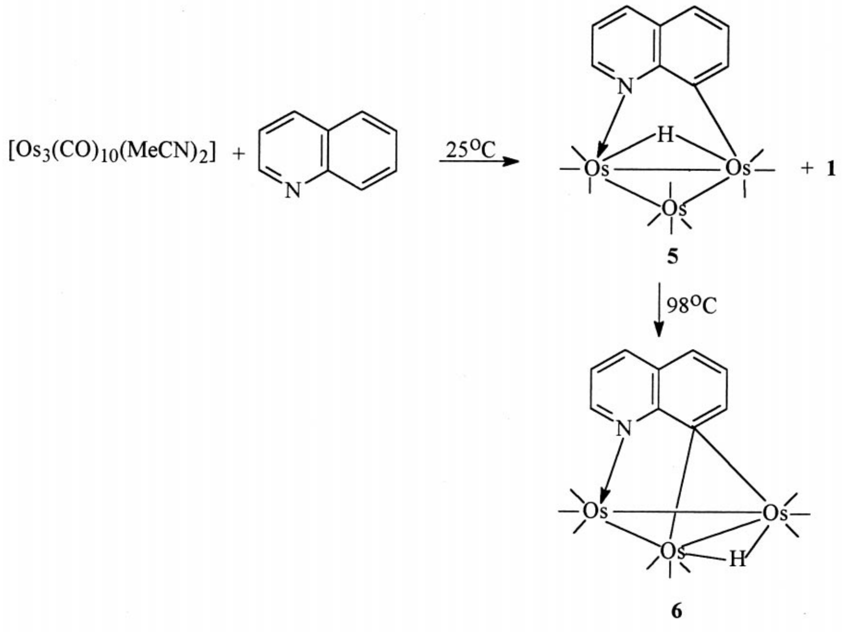

Scheme 2.

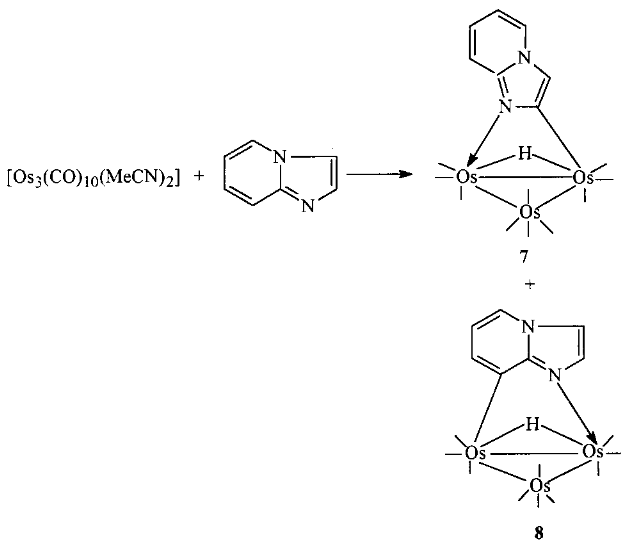

Scheme 3.

The IR spectrum of **7** in the carbonyl stretching region is similar to that of **1** [1], suggesting that they have structural similarities. The ^{1}H-NMR spectrum of **7** contains a singlet hydride resonance at δ −15.10 and two doublets at δ 7.92 and 7.01, two triplets at δ 7.28 and 6.70 and a singlet at δ 7.10, each integrating as one hydrogen atom. The doublets at δ 7.92 and 7.01 have been assigned to the C(4) and C(7) ring protons and the triplets at δ 7.28 and 6.70 have been assigned to the C(6) and C(5) ring protons, while the singlet at δ 7.10 is attributed to the C(3) ring proton. These assignments are consistent with the COSY correlations in 2D ^{1}H-NMR spectrum. The ^{1}H-NMR spectrum showed the absence of the C(2) proton that appears as a doublet at δ 7.48 in the spectrum of free imidazo(1,2-*a*)pyridine. Spectroscopic data indicated **7** as the most probable structure for this compound, and this was confirmed by an X-ray structure determination.

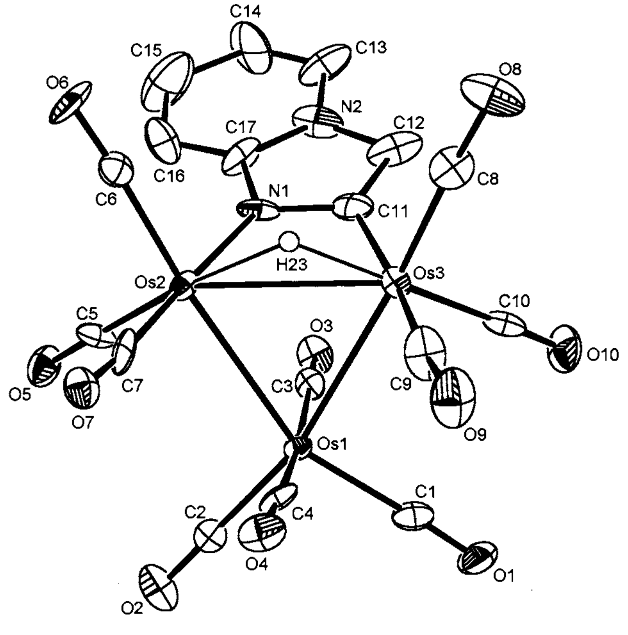

Fig. 1. Molecular structure of [(μ-H)$Os_3(CO)_{10}$(μ-1,2-η^2-$C_7H_5N_2$)] (**7**) showing the atom labeling scheme. Thermal ellipsoids are drawn at 40% probability level.

Table 1
Selected bond lengths (Å) and angles (°) for [$Os_3(CO)_{10}(H)(C_7H_5N_2)$] (**7**)

Bond lengths (Å)			
Os(1)–Os(2)	2.8644(10)	Os(1)–Os(3)	2.8898(11)
Os(2)–Os(3)	2.9736(10)	Os(2)–N(1)	2.134(11)
Os(3)–C(11)	2.10(2)	Os(2)–H(23)	1.73 [a]
Os(3)–H(23)	1.61 [a]	Os–C(CO)	1.909 [b]
C–O	1.154 [b]		
Bond angles (°)			
C(1)–Os(1)–C(3)	94.3(6)	C(1)–Os(1)–C(2)	100.7(6)
C(3)–Os(1)–C(2)	93.3(6)	C(1)–Os(1)–C(4)	91.9(6)
C(3)–Os(1)–C(4)	171.7(6)	C(2)–Os(1)–C(4)	91.0(6)
C(1)–Os(1)–Os(2)	154.6(5)	C(3)–Os(1)–Os(2)	84.8(4)
C(2)–Os(1)–Os(2)	104.7(4)	C(4)–Os(1)–Os(2)	87.3(4)
C(1)–Os(1)–Os(3)	92.4(5)	C(3)–Os(1)–Os(3)	85.7(5)
C(2)–Os(1)–Os(3)	166.9(4)	C(4)–Os(1)–Os(3)	88.5(5)
Os(2)–Os(1)–Os(3)	62.23(2)	C(5)–Os(2)–C(7)	91.6(6)
C(5)–Os(2)–C(6)	96.4(7)	C(7)–Os(2)–C(6)	92.2(6)
C(5)–Os(2)–N(1)	95.6(6)	C(7)–Os(2)–N(1)	172.7(6)
C(6)–Os(2)–N(1)	86.7(5)	C(5)–Os(2)–Os(1)	86.7(5)
C(7)–Os(2)–Os(1)	91.7(4)	C(6)–Os(2)–Os(1)	175.0(4)
N(1)–Os(2)–Os(1)	89.0(3)	C(5)–Os(2)–Os(3)	140.6(5)
C(7)–Os(2)–Os(3)	107.4(4)	C(6)–Os(2)–Os(3)	116.4(5)
N(1)–Os(2)–Os(3)	66.9(4)	Os(1)–Os(2)–Os(3)	59.30(3)
C(8)–Os(3)–C(9)	92.1(7)	C(8)–Os(3)–C(10)	96.4(7)
C(9)–Os(3)–C(10)	96.0(6)	C(8)–Os(3)–C(11)	88.3(6)
C(9)–Os(3)–C(11)	174.4(6)	C(10)–Os(3)–C(11)	89.5(6)
C(8)–Os(3)–Os(1)	175.4(5)	C(9)–Os(3)–Os(1)	88.9(5)
C(10)–Os(3)–Os(1)	87.9(5)	C(11)–Os(3)–Os(1)	90.2(4)
C(8)–Os(3)–Os(2)	117.0(5)	C(9)–Os(3)–Os(2)	106.2(5)
C(10)–Os(3)–Os(2)	138.4(5)	C(11)–Os(3)–Os(2)	68.7(4)
Os(1)–Os(3)–Os(2)	58.47(2)	Os(2)–H(23)–Os(3)	125.5 [a]
Os–C–O	176.8 [b]	C(17)–N(1)–C(11)	106.6(12)
C(17)–N(1)–Os(2)	140.1(12)	C(11)–N(1)–Os(2)	112.8(9)
N(1)–C(11)–C(12)	111.0(14)	N(1)–C(11)–Os(3)	111.6(10)
C(12)–C(11)–Os(3)	137.0(14)		

[a] The dimensions involving the hydride ligand are only approximate.

[b] Average values.

The molecular structure of **7** is shown in Fig. 1 with selected bond distances and angles in Table 1. The molecule consists of a triangular cluster of three osmium atoms with ten terminal carbonyl ligands distributed so that three are attached to each of Os(2) and Os(3) and four to Os(1). The three Os–Os distances are distinctly different [Os(2)–Os(3) = 2.9736(10), Os(1)–Os(2) = 2.8644(10) and Os(1)–Os(3) = 2.8898(11) Å] with the longest bond being associated with that spanned simultaneously by the hydride and the imidazo(1,2-*a*)pyridine ligand. The average Os–Os separation of 2.9093 Å is somewhat longer than the average Os–Os distances of 2.877(3) Å found in [$Os_3(CO)_{12}$] [26]. The arrangements of the ligands around the metal triangle in **7** are similar to those found in the related quinoline (C_9H_7N) and phenanthridine ($C_{13}H_9N$) clusters $[(\mu\text{-H})Os_3(CO)_{10}(\mu\text{-}1,2\text{-}\eta^2\text{-}C_9H_6N)]$ [1], $[(\mu\text{-H})Ru_3(CO)_{10}(\mu\text{-},2\text{-}\eta^2\text{-}C_9H_6N)]$ [27] and $[(\mu\text{-H})Ru_3(CO)_{10}(\mu\text{-}1,2\text{-}\eta^2\text{-}C_{13}H_8N)]$ [2]. As in these complexes, the molecular plane containing the imidazo(1,2-*a*)pyridine ligand in **7** is also nearly perpendicular to the osmium triangle as shown by the values of 89.0(3) and 90.2(4)° for the angles N(1)–Os(2)–Os(1) and C(11)–Os(3)–Os(1), respectively. The C(11)–N(1) bond length of 1.37(2) Å is within the range found for other related compounds with coordinated heterocycles, e.g. 1.367–1.383 Å in $[(\mu\text{-H})_2Os_3(CO)_8(\mu\text{-}1,2\text{-}\eta^2\text{-}C_9H_6N)_2$ [1], 1.329 Å in $[(\mu\text{-H})Os_3(CO)_{10}(\mu\text{-}1,2\text{-}\eta^2\text{-}C_9H_6N)]$ [1], and 1.38(2) Å in $[(\mu\text{-H})Ru_3(CO)_{10}(\mu\text{-}1,2\text{-}\eta^2\text{-}C_9H_6N)]$ [27]. The Os(3)–C(11) and Os(2)–N(1) distances of 2.10(2) and 2.134(11) Å, respectively are similar to the corresponding values in the above quinoline and phenanthridine complexes.

The ν(CO) stretches of **8** are very similar to those of the recently reported quinoline analog **5** [25], suggesting that the two compounds have similar structural arrangements. The ^{1}H-NMR spectrum of **8** contains two doublets and a triplet at δ 7.71, 7.66 and 6.64 due to the C(6), C(5) and C(4) protons of the pyridine ring, two singlets at δ 7.35 and 7.34 due to the C(3) and C(2) protons of the imidazole ring and a singlet resonance at δ −14.24 due to the bridging hydride ligand. The ^{1}H-NMR spectrum does not contain the expected resonance for the C(7) proton of the pyridyl ring which leads to the suggestion that it has the structure **8**. These assignments are based on the correlation pattern in the 2D COSY ^{1}H-NMR spectrum of **8**. There are very few examples of decacarbonyl triosmium complexes containing bicyclic heterocyclic ligands in which both the rings of the heterocycle are coordinated as in **8**. One recent example is the quinoline derivative **5** but this compound has not been structurally characterized. Unambiguous proof of the structure of **8** has now been obtained from a single-crystal X-ray diffraction study.

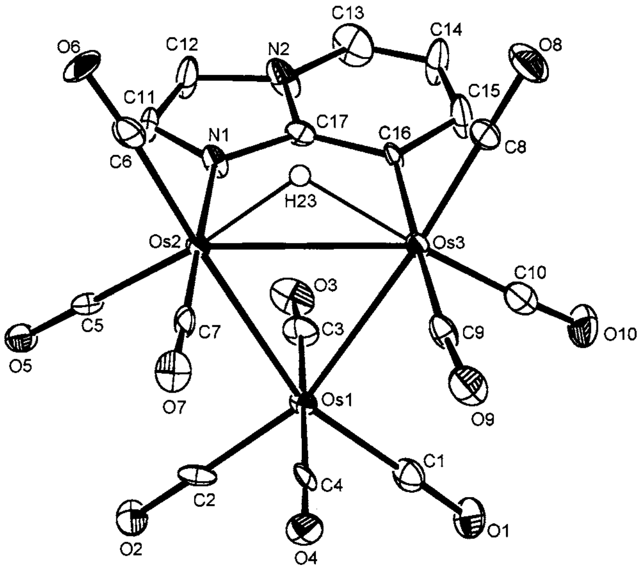

Fig. 2. Molecular structure of $[(\mu\text{-H})Os_3(CO)_{10}(\mu\text{-}1,7\text{-}\eta^2\text{-}C_7H_5N_2)]$ (**8**) showing the atom labeling scheme. Thermal ellipsoids are drawn at 40% probability level.

Table 2
Selected bond lengths (Å) and angles (°) for $[Os_3(CO)_{10}(H)(C_7H_5N_2)]$ (**8**)

Bond lengths (Å)			
Os(1)–Os(2)	2.8794(7)	Os(1)–Os(3)	2.9001(8)
Os(2)–Os(3)	2.9654(9)	Os(2)–N(1)	2.126(9)
Os(2)–H(23)	1.72 [a]	Os(3)–C(16)	2.120(11)
Os(3)–H(23)	1.93 [a]	Os–C(CO)	1.898 [b]
C–O	1.155 [b]		
Bond angles (°)			
C(3)–Os(1)–C(1)	91.5(5)	C(2)–Os(1)–C(1)	102.4(6)
C(2)–Os(1)–C(3)	91.4(5)	C(1)–Os(1)–C(4)	90.3(5)
C(3)–Os(1)–C(4)	177.5(5)	C(2)–Os(1)–C(4)	89.9(5)
C(1)–Os(1)–Os(2)	158.8(4)	C(3)–Os(1)–Os(2)	88.5(4)
C(2)–Os(1)–Os(2)	98.8(4)	C(4)–Os(1)–Os(2)	89.2(3)
C(2)–Os(1)–Os(3)	160.5(4)	C(3)–Os(1)–Os(3)	87.7(4)
C(1)–Os(1)–Os(3)	97.0(4)	C(4)–Os(1)–Os(3)	90.4(3)
Os(2)–Os(1)–Os(3)	61.74(2)	C(5)–Os(2)–C(7)	92.6(5)
C(5)–Os(2)–C(6)	96.4(5)	C(7)–Os(2)–C(6)	91.0(5)
C(5)–Os(2)–N(1)	89.8(4)	C(7)–Os(2)–N(1)	177.3(5)
C(6)–Os(2)–N(1)	87.5(5)	C(5)–Os(2)–Os(1)	85.6(3)
C(7)–Os(2)–Os(1)	89.6(4)	C(6)–Os(2)–Os(1)	177.9(4)
N(1)–Os(2)–Os(1)	91.8(3)	C(5)–Os(2)–Os(3)	143.9(4)
C(7)–Os(2)–Os(3)	95.5(3)	C(6)–Os(2)–Os(3)	118.5(4)
N(1)–Os(2)–Os(3)	83.2(3)	Os(1)–Os(2)–Os(3)	59.47(2)
C(8)–Os(3)–C(10)	97.7(6)	C(8)–Os(3)–C(9)	95.3(5)
C(10)–Os(3)–C(9)	92.3(5)	C(8)–Os(3)–C(16)	84.2(5)
C(10)–Os(3)–C(16)	86.7(5)	C(9)–Os(3)–C(16)	178.8(5)
C(8)–Os(3)–Os(1)	175.8(4)	C(10)–Os(3)–Os(1)	86.1(4)
C(9)–Os(3)–Os(1)	86.2(4)	C(16)–Os(3)–Os(1)	94.3(3)
C(8)–Os(3)–Os(2)	117.1(4)	C(10)–Os(3)–Os(2)	142.8(4)
C(9)–Os(3)–Os(2)	96.8(4)	C(16)–Os(3)–Os(2)	84.4(3)
Os(1)–Os(3)–Os(2)	58.79(2)	Os(2)–H(23)–Os(3)	108.7 [a]
C(17)–N(1)–Os(2)	123.0(8)	C(11)–N(1)–Os(2)	130.0(9)
C(17)–N(1)–C(11)	107.0(10)	C(15)–C(16)–Os(3)	127.9(9)
C(17)–C(16)–Os(3)	120.4(8)	C(15)–C(16)–C(17)	111.7(10)
Os–C–O	176.4 [b]		

[a] The dimensions involving the hydride ligand are only approximate.

[b] Average values.

The molecular structure of **8** is shown in Fig. 2 and selected bond distances and angles are presented in Table 2. The structure consists of a triangular metal core with three distinct metal–metal bond distances [Os(2)–Os(3) = 2.9654(9), Os(1)–Os(3) = 2.9001(8) and Os(1)–Os(2) = 2.8794(7) Å] with ten terminal carbonyl groups distributed as in **7**. The doubly bridged Os(2)–Os(3) bond is again significantly longer than the unbridged Os(1)–Os(2) and Os(1)–Os(3) bonds, a pattern also observed in **7**. The average Os–Os distance of 2.9150 Å is slightly longer than that in **7**. The heterocyclic ligand in **8** donates three electrons to the cluster via a two-electron donor bond from N(1) to Os(2) [Os(2)–N(1) = 2.126(9) Å] and one-electron σ bond

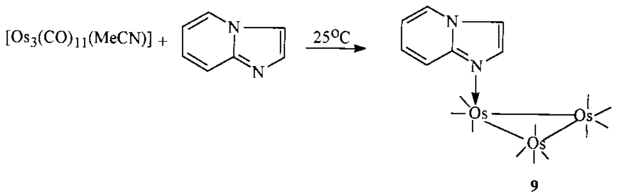

Scheme 4.

from C(16) to Os(3) [Os(3)–C(16) = 2.120(11) Å]. The basic structure of this compound is similar to that adopted by **7** with the activation of the C(7)–H bond instead of the C(2)–H bond of the imidazole ring as in **7**. These two compounds reveal an interesting example of 'linkage isomerism', where the modes of bonding of the imidazo(1,2-*a*)pyridine heterocyle are totally different.

In order to isolate the N-coordinated intermediate (before the cyclometalation occurs) we decided to explore the reactivity of imidazo(1,2-*a*)pyridine with $[Os_3(CO)_{11}(MeCN)]$. It was observed that the monoacetonitrile compound reacts smoothly with imidazo(1,2-*a*)pyridine at 25°C to afford $[Os_3(CO)_{11}(\eta^1\text{-}C_7H_6N_2)]$ (**9**) in 58% yield (Scheme 4). The same compound was also obtained in similar yield starting the reaction from $[Os_3(CO)_{12}]$ and imidazo(1,2-*a*)pyridine in the presence of Me_3NO at 60°C.

Compound **9** has been characterized by elemental analysis, IR and ^{1}H-NMR spectroscopy and X-ray diffraction analysis. The close similarity of the ν(CO) stretching frequencies of **9** to those of $[Os_3(CO)_{11}(\eta^1\text{-}C_5H_5N)]$ [28], $[Os_3(CO)_{11}(MeCN)]$ [29] and $[Os_3(CO)_{11}(\eta^1\text{-}CH{=}NCH{=}CHNH)]$ [21] suggests that the compounds are structurally analogous. The ^{1}H-NMR spectrum of **9** in the δ 0–10 region contains six well-separated resonances, each integrating for one hydrogen atom. These data are consistent with the results of an X-ray study.

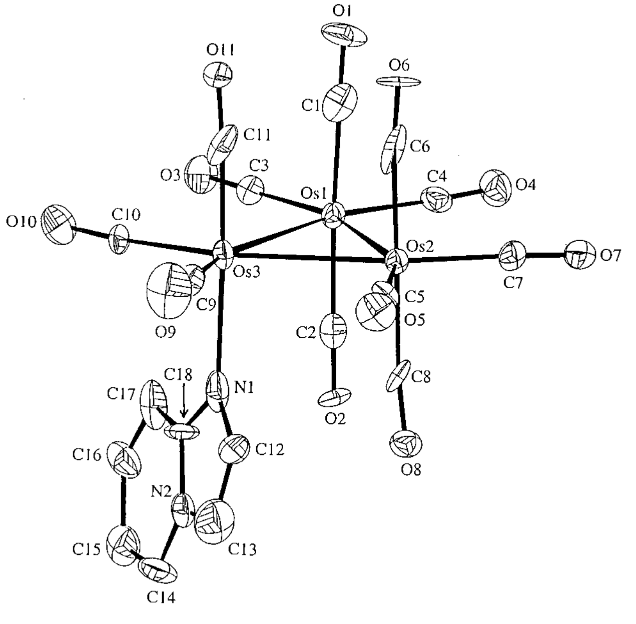

Fig. 3. Molecular structure of $[Os_3(CO)_{11}(\eta^1\text{-}C_7H_6N_2)]$ (**9**) showing the atom labeling scheme. Thermal ellipsoids are drawn at 40% probability level.

The X-ray structure of **9** is shown in Fig. 3 and selected bond distances and angles are given in Table 3. The molecule consists of a triangular cluster of three osmium atoms without any bridging ligands. The 11 carbonyl groups and the imidazo(1,2-*a*)pyridine ligand are all terminally bonded. The metal–metal bonds [Os(1)–Os(2) = 2.8802(10), Os(1)–Os(3) = 2.8906(11) and Os(2)–Os(3) = 2.8722(11) Å] are nearly equal and the average value (2.8810 Å) is comparable to that in $[Os_3(CO)_{12}]$ (2.877 Å) [26]. The organic ligand is coordinated to Os(3) through the imino nitrogen atom and occupies an axial coordination site. The Os(1)–N(1) distance at 2.25(2) Å is significantly longer than the values in **7**, **8**, **11** and also $[Os_3(CO)_{11}(MeCN)]$ (2.074(22) Å) [29], but comparable to those in $[Os_3(CO)_{11}(\eta^1\text{-}CH{=}NCH{=}CHNH)]$ (2.23(2) Å) [21] and $[(\mu\text{-}H)_2Os_5(CO)_{14}(\eta^1\text{-}C_5H_5N)]$ (2.214(22) Å) [30].

Table 3
Selected bond lengths (Å) and angles (°) for $[Os_3(CO)_{11}(C_7H_6N_2)]$ (**9**)

Bond lengths (Å)			
Os(1)–Os(2)	2.8802(10)	Os(1)–Os(3)	2.8906(11)
Os(2)–Os(3)	2.8722(11)	Os(3)–N(1)	2.25(2)
Os–C(CO)	1.924 [a]	C–O	1.143 [a]
Bond angles (°)			
Os(2)–Os(1)–Os(3)	59.70(3)	Os(3)–Os(2)–Os(1)	60.33(3)
Os(2)–Os(3)–Os(1)	59.97(3)	C(3)–Os(1)–C(4)	105.4(7)
C(3)–Os(1)–C(1)	91.8(7)	C(4)–Os(1)–C(1)	88.4(8)
C(3)–Os(1)–C(2)	92.6(7)	C(4)–Os(1)–C(2)	90.8(7)
C(1)–Os(1)–C(2)	175.6(6)	C(3)–Os(1)–Os(2)	156.0(5)
C(4)–Os(1)–Os(2)	98.5(5)	C(1)–Os(1)–Os(2)	88.3(5)
C(2)–Os(1)–Os(2)	87.6(5)	C(3)–Os(1)–Os(3)	96.4(5)
C(4)–Os(1)–Os(3)	158.2(5)	C(1)–Os(1)–Os(3)	91.6(6)
C(2)–Os(1)–Os(3)	87.5(5)	C(5)–Os(2)–C(7)	106.2(7)
C(5)–Os(2)–C(6)	88.6(7)	C(7)–Os(2)–C(6)	91.9(8)
C(5)–Os(2)–C(8)	90.3(7)	C(7)–Os(2)–C(8)	88.8(7)
C(6)–Os(2)–C(8)	178.8(7)	C(5)–Os(2)–Os(3)	93.1(5)
C(7)–Os(2)–Os(3)	160.7(5)	C(6)–Os(2)–Os(3)	89.3(5)
C(8)–Os(2)–Os(3)	90.3(5)	C(5)–Os(2)–Os(1)	153.4(5)
C(7)–Os(2)–Os(1)	100.4(5)	C(6)–Os(2)–Os(1)	90.9(5)
C(8)–Os(2)–Os(1)	89.9(4)	C(11)–Os(3)–C(10)	88.3(8)
C(11)–Os(3)–C(9)	89.7(9)	C(10)–Os(3)–C(9)	100.7(8)
C(11)–Os(3)–N(1)	174.7(7)	C(10)–Os(3)–N(1)	91.1(7)
C(9)–Os(3)–N(1)	85.2(7)	C(11)–Os(3)–Os(2)	90.5(6)
C(10)–Os(3)–Os(2)	161.5(6)	C(9)–Os(3)–Os(2)	97.8(5)
N(1)–Os(3)–Os(2)	91.7(4)	C(11)–Os(3)–Os(1)	87.8(7)
C(10)–Os(3)–Os(1)	101.5(6)	C(9)–Os(3)–Os(1)	157.6(6)
N(1)–Os(3)–Os(1)	97.5(4)	C(18)–N(1)–Os(3)	129.1(12)
C(12)–N(1)–Os(3)	123.9(13)	C(18)–N(1)–C(12)	106(2)
Os–C–O	176.2 [a]		

[a] Average value.

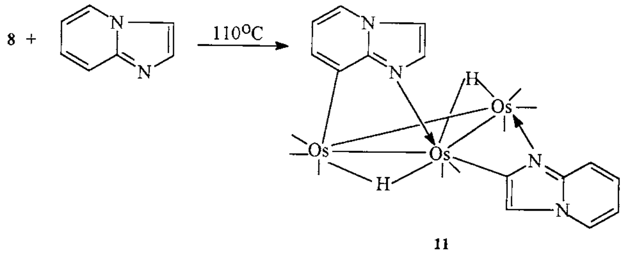

Scheme 5.

As expected, thermolysis of **9** in octane at 128°C gives the isomeric decacarbonyl compounds **7** and **8** in 32 and 15% yields, respectively. The major product is formed by activation of the C(2)–H bond of the pyridine ring, while the minor product is formed by C(7)–H bond activation of the imidazole ring. These results show that the formation of **7** and **8** from the reaction shown in Scheme 3 most probably proceeds via initial formation of the N-coordinated intermediate followed by activation of the C(2)–H or C(7)–H bonds with the metal and subsequent hydride transfer to the metal. We explored the substitution reactions of **9** with two-electron donor ligands such as PPh_3, $P(OMe)_3$, and ^{t}BuNC. Treatment of a dichloromethane solution of **9** with excess L (L = PPh_3, $P(OMe)_3$ or ^{t}BuNC) results in the formation of the known compounds $[Os_3(CO)_{11}(L)]$ in high yields (L = PPh_3, 85%; L = $P(OMe)_3$, 82%; L = ^{t}BuNC = 83%) by displacement of the imidazo(1,2-*a*)pyridine ligand [28]. These results demonstrate that the coordinated imidazo(1,2-*a*)pyridine ligand in **9** is labile and easily displaced by two-electron donor ligands exhibiting behavior similar to $[Os_3(CO)_{11}(MeCN)]$ [28], $[Os_3(CO)_{10}(MeCN)_2]$ [28], $[Os_3(CO)_{11}\{\eta^1\text{-}SC(NMe_2)_2]$ [31] and $[Os_3(CO)_9\text{-}(\mu\text{-}OH)(\mu\text{-}MeOCO)\{\eta^1\text{-}SC(NMe_2)_2\}]$ [32].

In contrast to the quinoline compound **5**, which decarbonylates both thermally and photochemically to **6**, compound **8** is surprisingly stable to thermal and photochemical decarbonylation without showing any further reactivity towards nucleophiles at ambient temperatures. However, a further reaction of **8** with imidazo(1,2-*a*)pyridine affords $[(\mu\text{-}H)_2Os_3(CO)_8(\mu\text{-}1,7\text{-}\eta^2\text{-}C_7H_5N_2)(\mu\text{-}1,2\text{-}\eta^2\text{-}C_7H_5N_2)]$ (**11**) (Scheme 5), containing two heterocyclic ligands, in a 45% yield. Compound **11** has been characterized by elemental analysis, IR and ^{1}H-NMR spectroscopic data and single-crystal diffraction analysis.

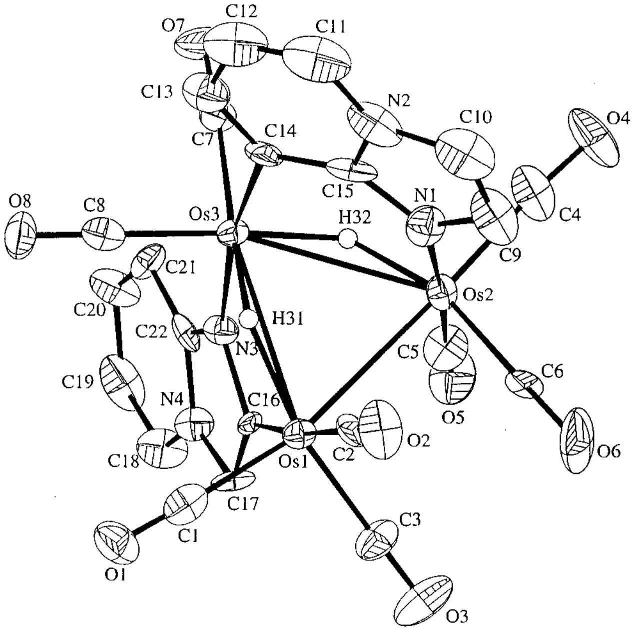

Fig. 4. Molecular structure of $[(\mu\text{-}H)_2Os_3(CO)_8(\mu\text{-}1,7\text{-}\eta^2\text{-}C_7H_5N_2)(\mu\text{-}1,2\text{-}\eta^2\text{-}C_7H_5N_2]$ (**11**) showing the atom labeling scheme. Thermal ellipsoids are drawn at 40% probability level.

The molecular structure of **11** is shown in Fig. 4 and selected bond distances and angles data are presented in Table 4. The cluster consists of an Os_3 triangle with two imidazo(1,2-*a*)pyridine derived ligands forming bridges between two different Os–Os edges and with different coordination modes; one is coordinated via the imino nitrogen and C(2) carbon atoms giving dimetallaazacyclopentene, whereas the other coordinates via the imino nitrogen and C(7) carbon atoms providing a dimetallaazacyclobutene. The two coordination modes of the imidazo(1,2-*a*)pyridyl ligands are similar to those observed in **7** and **8**, respectively. Atom Os(3) is coordinated to two heterocyclic ligands and two CO ligands, whereas the atoms Os(1) and Os(2) are each bonded to one heterocyclic ligand and three CO ligands. The two Os–Os edges accommodating the $C_7H_5N_2$ and the hydride bridges [Os(2)–Os(3) = 3.0242(11), Os(1)–Os(3) = 3.0352(12) Å] are longer than the nonbridged edge [Os(1)–Os(2) = 2.8642(11) Å]. These Os–Os distances are close to the respective values reported for $[(\mu\text{-}H)_2Os_3(CO)_8(\mu\text{-}\eta^2\text{-}C_6H_4CH_2C{=}N)_2]$ (2.950(1) and 2.956(1) Å for the doubly bridged edges and 2.861(1) Å for the nonbridged edge) [20]. The organic ligands lie, respectively above and below the metal plane, as do the hydride ligands, each opposite its corresponding organic ligand. The Os–N [Os(2)–N(1) = 2.14(2), Os(3)–N(3) = 2.113(13) Å] and Os–C [Os(3)–C(14) = 2.08(2), Os(1)–C(16) = 2.10(2) Å] bond distances are comparable to the corresponding values in **7** and **8**, but are shorter than those in **11**. The geometry parameters associated with the imidazo(1,2-*a*)pyridyl units in the four compounds reported here are as expected for this type of ligand, with only minor differences in some angles at the atoms involved in coordination with the metal centers. The dimensions of the Os–C–O units in all the complexes are also very similar. It may be noted that only a few trimetallic clusters containing two N-heterocyclic derived ligands have been structurally characterized and reported in the literature. Examples of these type of complexes include $[(\mu\text{-}H)_2Ru_3(CO)_8(\mu\text{-}\eta^2\text{-}$

Table 4
Selected bond lengths (Å) and angles (°) for $[Os_3(CO)_8(H)_2(C_7H_5N_2)_2]$ (**11**)

Bond lengths (Å)			
Os(1)–Os(2)	2.8642(11)	Os(1)–Os(3)	3.0352(12)
Os(2)–Os(3)	3.0242(12)	Os(1)–C(16)	2.10(2)
Os(1)–H(31)	1.79 [a]	Os(2)–N(1)	2.14(2)
Os(2)–H(32)	1.68 [a]	Os(3)–C(14)	2.08(2)
Os(3)–N(3)	2.113(13)	Os(3)–H(31)	1.63 [a]
Os(3)–H(32)	1.72 [a]	Os–C(CO)	1.903 [b]
C–O	1.14 [b]		
Bond angles (°)			
C(3)–Os(1)–C(1)	97.2(7)	C(3)–Os(1)–C(2)	93.9(7)
C(1)–Os(1)–C(2)	96.0(7)	C(3)–Os(1)–C(16)	88.9(7)
C(1)–Os(1)–C(16)	89.0(6)	C(2)–Os(1)–C(16)	173.9(5)
C(3)–Os(1)–Os(2)	95.1(5)	C(1)–Os(1)–Os(2)	167.5(4)
C(2)–Os(1)–Os(2)	85.4(4)	C(16)–Os(1)–Os(2)	89.0(3)
C(3)–Os(1)–Os(3)	145.7(6)	C(1)–Os(1)–Os(3)	106.3(4)
C(2)–Os(1)–Os(3)	107.8(4)	C(16)–Os(1)–Os(3)	67.4(3)
Os(2)–Os(1)–Os(3)	61.60(3)	C(6)–Os(2)–C(5)	92.3(7)
C(6)–Os(2)–C(4)	99.1(6)	C(5)–Os(2)–C(4)	94.7(8)
C(6)–Os(2)–N(1)	91.3(6)	C(5)–Os(2)–N(1)	175.6(6)
C(4)–Os(2)–N(1)	87.3(7)	C(6)–Os(2)–Os(1)	82.8(4)
C(5)–Os(2)–Os(1)	85.8(5)	C(4)–Os(2)–Os(1)	178.0(5)
N(1)–Os(2)–Os(1)	92.1(3)	C(6)–Os(2)–Os(3)	142.9(4)
C(5)–Os(2)–Os(3)	96.2(5)	C(4)–Os(2)–Os(3)	116.0(5)
N(1)–Os(2)–Os(3)	79.4(3)	Os(1)–Os(2)–Os(3)	61.98(3)
C(8)–Os(3)–C(7)	90.2(6)	C(8)–Os(3)–C(14)	91.3(6)
C(7)–Os(3)–C(14)	87.6(7)	C(8)–Os(3)–N(3)	95.0(6)
C(7)–Os(3)–N(3)	101.0(6)	C(14)–Os(3)–N(3)	169.3(5)
C(8)–Os(3)–Os(2)	157.9(4)	C(7)–Os(3)–Os(2)	111.4(4)
C(14)–Os(3)–Os(2)	85.1(4)	N(3)–Os(3)–Os(2)	85.8(3)
C(8)–Os(3)–Os(1)	103.7(4)	C(7)–Os(3)–Os(1)	162.1(5)
C(14)–Os(3)–Os(1)	103.2(4)	N(3)–Os(3)–Os(1)	66.9(3)
Os(2)–Os(3)–Os(1)	56.42(2)	Os(1)–H(31)–Os(3)	125.3 [a]
Os(2)–H(32)–Os(3)	125.7 [a]	C(15)–N(1)–C(9)	107(2)
C(15)–N(1)–Os(2)	124.8(11)	C(9)–N(1)–Os(2)	127.1(12)
C(16)–N(3)–C(22)	107.3(12)	C(16)–N(3)–Os(3)	113.0(11)
C(22)–N(3)–Os(3)	139.5(10)	C(13)–C(14)–C(15)	111(2)
C(13)–C(14)–Os(3)	129.4(12)	C(15)–C(14)–Os(3)	119.3(12)
C(17)–C(16)–N(3)	108.6(14)	C(17)–C(16)–Os(1)	138.6(10)
N(3)–C(16)–Os(1)	112.7(11)		

[a] The parameters involving the hydride ligands are only approximate.

[b] Average values.

$C_5H_4N)_2]$ [33], $[(\mu\text{-}H)_2Os_3(CO)_8(\mu\text{-}\eta^2\text{-}C{=}NCH_2CH_2CH_2)_2]$ [34], $[(\mu\text{-}H)_2Os_3(CO)_8(\mu\text{-}\eta^2\text{-}C_6H_4CH_2\text{-}C{=}N)_2]$ [20] and $[(\mu\text{-}H)_2Os_3(CO)_8(\mu\text{-}\eta^2\text{-}C_9H_6N)_2]$ [1]. All these compounds contain the two heterocyclic ligands in the same bond- ing mode unlike compound **11**, where the two heterocyclic ligands involve different coordination modes. The ^{1}H-NMR spectrum of **11** contains two equal intensity hydride resonances at δ −11.49 and −13.66 as well-separated resonances for the ten protons of the two heterocyclic ligands, which is consistent with the X-ray structure.

The reaction of **7** with excess imidazo(1,2-*a*)pyridine at 110°C yields the bis{imidazo(1,2-*a*)pyridine} compound $[(\mu\text{-}H)_2Os_3(CO)_8(\mu\text{-}1,2\text{-}\eta^2\text{-}C_7H_5N_2)_2]$ (**10**) (Scheme 6) in a 34% yield. It is proposed that the two heterocyclic ligands bridge through the imino nitrogen and C(2) carbon.

The structure proposed for **10** is based on elemental analysis, IR and ^{1}H-NMR spectroscopy, but could not be confirmed by X-ray studies due to the lack of suitable single crystals. The IR spectrum of this compound is very similar to those for the structurally characterized compounds $[(\mu\text{-}H)_2Os_3(CO)_8(\mu\text{-}\eta^2\text{-}C_6H_4CH_2C{=}N)_2]$ [20], $[(\mu\text{-}H)_2Os_3(CO)_8(\mu\text{-}\eta^2\text{-}C{=}NCH_2CH_2CH_2)_2]$ [34] and $[(\mu\text{-}H)_2Os_3(CO)_8(\mu\text{-}\eta^2\text{-}NC_5H_4)_2]$ [35]. The ^{1}H-NMR spectrum of **10** contains two hydride resonances at δ −11.66 and −13.18 with an integrated ratio of 1:1 and three multiplets at δ 7.78, 7.57 and 6.68, two singlets at δ 7.15 and 7.07 and a doublet at δ 7.95 in a 3:2:2:1:1:1 intensity ratio, respectively. The singlets at δ 7.15 and 7.07, assigned to the C(3)–H protons of the heterocyclic ligands, may be compared with that at δ 7.10 found in **7**. The resonances of the remaining protons overlap and, therefore, have not been assigned. Spectroscopic data do suggest that each $C_7H_5N_2$ ligand is doubly bridging and is bonded to the osmium through a σ Os–C bond adjacent to the coordinated imino nitrogen atom as in the three compounds mentioned above.

Both **7** and **8** react with PPh_3 at 110°C to give the mono-substituted derivatives $[(\mu\text{-}H)Os_3(CO)_9(\mu\text{-}1,2\text{-}\eta^2\text{-}C_7H_5N_2)(PPh_3)]$ (**12**) and $[(\mu\text{-}H)Os_3(CO)_9(\mu\text{-}1,7\text{-}\eta^2\text{-}C_7H_5N_2)(PPh_3)]$ (**13**) (Scheme 7) in 47 and 45% yields, respectively. These compounds have been characterized by ^{1}H- and ^{31}P-NMR, IR and elemental analysis. The ν(CO) stretches of **12** and **13** are very close to those reported for the structurally characterized compound $[(\mu\text{-}H)Os_3(CO)_9(\mu\text{-}\eta^2\text{-}C{=}NCH_2CH_2CH_2)(PPh_3)]$ [36], suggesting that they adopt very similar structures. In the ^{1}H-NMR spectra, in addition to the well-separated resonances for the phenyl protons of the PPh_3 ligands and ring protons of the heterocyclic ligands, each of **12** and **13** contains a doublet resonance for the hydride (δ −14.71, $J = 11.8$ Hz for **12**; δ −13.85, $J = 15.3$ Hz for **13**), which becomes a singlet in the phosphorus-decoupling spectrum and is consistent with the proposed

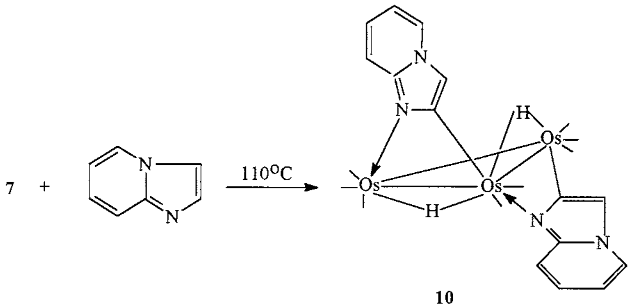

10

Scheme 6.

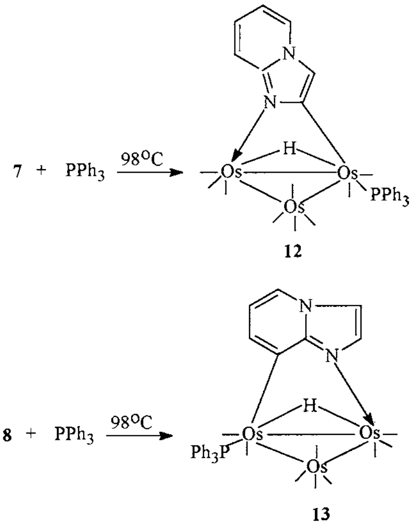

Scheme 7.

structures. The $^{31}P\{^1H\}$-NMR spectra of both **12** and **13** contain a singlet (δ 9.5 for **12**; δ 11.4 for **13**) and accord with the proposed structures. The ^1H- and $^{31}P\{^1H)$-NMR spectroscopic data and the magnitude of the phosphorus hydrogen couplings are very similar to those observed for the related phosphine substituted clusters $[(\mu\text{-H})Os_3(CO)_9(\mu\text{-}\eta^2\text{-C=NCH}_2CH_2CH_2CH_2)(PPh_3)]$ [12] and $[(\mu\text{-H})Os_3(CO)_9(\mu\text{-}\eta^2\text{-C=NCH}_2CH_2CH_2)(PPh_3)]$ [36] in which the phosphine and the hydride ligands are coordinated to the same metal.

3. Experimental

All the reactions were carried out under an atmosphere of purified nitrogen using standard Schlenk techniques. Solvents were distilled from the appropriate drying agents and stored under nitrogen. IR spectra were recorded on a Shimadzu 8101 spectrophotometer. ^1H- and $^{31}P\{^1H\}$-NMR spectra were recorded on a Bruker AC 200 or Bruker AC 250 or Varian Unity Plus 400 spectrometer and calibrated against internal $Me_4Si\{^1H\}$ or external $H_3PO_4\{^{31}P\}$. Elemental analyses were performed in the Analytical Laboratories of the University of Freiburg. $[Os_3(CO)_{11}(MeCN)]$ and $[Os_3(CO)_{10}(MeCN)_2]$ were prepared according to published methods [28]. Imidazo(1,2-*a*)pyridine, triphenylphosphine, trimethyl phosphite and *tert*-butyl isocanide were purchased from Aldrich.

3.1. Reaction of $[Os_3(CO)_{11}(MeCN)]$ with imidazo(1,2-a) pyridine

A CH_2Cl_2 solution (2 cm^3) of imidazo(1,2-*a*)pyridine (0.051 g, 0.432 mmol) was added dropwise to a CH_2Cl_2 solution (30 cm^3) of $[Os_3(CO)_{11}(MeCN)]$ (0.130 g, 0.140 mmol) and stirred for 12 h. The solvent was then removed in vacuo and the residue chromatogaphed by TLC on silica gel. Elution with hexane–CH_2Cl_2 (3:1, v/v) gave one major band which yielded $[Os_3(CO)_{11}(\eta^1\text{-}C_7H_6N_2)]$ (**9**) (0.077g, 58%) as yellow crystals after recrystallization from hexane–CH_2Cl_2 at −20°C. (Found: C, 21.74; H, 0.62; N, 2.80. $C_{18}H_6N_2O_{11}Os_3$ requires: C, 21.69; H, 0.61; N, 2.81%). IR (ν(CO), CH_2Cl_2): 2104s, 2049s, 2033s, 2008vs, 1992sh, 1971m, 1957sh cm^{-1}; ^1H-NMR ($CDCl_3$): δ 8.13 (d, 1H, $J = 6.4$ Hz), 7.71 (d, 1H, $J = 6.4$ Hz), 7.64 (s, 1H), 7.53 (s, 1H), 7.50 (t, 1H, $J = 6.4$ Hz), 6.79 (t, 1H, $J = 6.4$ Hz).

3.2. Reaction of $[Os_3(CO)_{12}]$ with imidazo(1,2-a)pyridine

$[Os_3(CO)_{12}]$ (0.105 g, 0.116 mmol), imidazo(1,2-*a*)pyridine (0.065 g, 0.55 mmol) and benzene (60 cm^3) were mixed in a three-necked round-bottom flask. The resulting suspension was heated to 60°C and a methanolic solution (2 cm^3) of Me_3NO (0.010 g, 0.113 mmol) was added dropwise. The reaction mixture was heated to 60°C for an additional 2 h. The solvent was removed under reduced pressure and the residue chromatographed by TLC on silica gel. Elution with hexane–CH_2Cl_2 (3:1, v/v) gave one major band, which yielded **9** (0.069 g, 60%) as yellow crystals after recrystallization from hexane–CH_2Cl_2 at −20°C.

3.3. Reaction of $[Os_3(CO)_{10}(MeCN)_2]$ with imidazo(1,2-a)pyridine

A solution of $[Os_3(CO)_{10}(MeCN)_2]$ (0.185 g, 0.198 mmol) and imidazo(1,2-*a*)pyridine (0.130 g, 1.10 mmol) in CH_2Cl_2 (30 cm^3) was stirred for 24 h. The solvent was removed under reduced pressure and the residue chromatographed by TLC on silica gel. Elution with hexane–CH_2Cl_2 (3.1, v/v) gave two bands. The faster moving band afforded $[(\mu\text{-H})Os_3(CO)_{10}(\mu\text{-}1,2\text{-}\eta^2\text{-}C_7H_5N_2)]$ (**7**) (0.058 g, 30%) as yellow crystals after recrystallization from hexane–CH_2Cl_2 at −20°C. (Found: C, 20.20; H, 0.59; N, 2.99. $C_{17}H_6N_2O_{10}Os_3$ requires: C, 21.08; H, 0.62; N, 2.89%). IR (ν(CO), hexane): 2103m, 2063vs, 2052vs, 2021vs, 2008vs, 2000m, 1990s, 1974w cm^{-1}; ^1H-NMR ($CDCl_3$): δ 7.92 (d, 1H, $J = 6.7$ Hz), 7.28 (t, 1H, $J = 6.4$ Hz), 7.10 (s, 1H), 7.01 (d, 1H, $J = 6.7$ Hz), 6.70 (t, 1H, $J = 6.7$ Hz), −15.10 (s, 1H). The slower moving band gave $[(\mu\text{-H})Os_3(CO)_{10}(\mu\text{-}1,7\text{-}\eta^2\text{-}C_7H_5N_2)]$ (**8**) (0.077 g, 40%) as yellow crystals after recrystallization from hexane–CH_2Cl_2 at −20°C. (Found: C, 21.15; H, 0.63; N, 2.93. $C_{17}H_6N_2O_{10}Os_3$ requires: C, 21.08; H, 0.62; N, 2.89%). IR (ν(CO), hexane): 2103m, 2062vs, 2052vs, 2021vs, 2005vs, 1991s, 1973w cm^{-1}; ^1H-NMR ($CDCl_3$): δ 7.71 (d, 1H, $J = 6.4$ Hz), 7.66 (d, 1H, $J = 6.4$ Hz), 7.35 (s, 1H), 7.34 (s, 1H), 6.64 (t, 1H, $J = 6.4$ Hz), −14.24 (s, 1H).

3.4. Reaction of **9** with PPh_3

To a CH_2Cl_2 solution (20 cm^3) of **9** (0.040 g, 0.040 mmol) was added PPh_3 (0.021 g, 0.080 mmol) and the reaction mixture was stirred for 12 h. The solvent was rotary evaporated and the residue chromatographed by TLC on silica gel. Elution with hexane–CH_2Cl_2 (5:1, v/v) gave one major band which yielded $[Os_3(CO)_{11}(PPh_3)]$ (0.039 g, 85%).

3.5. Reaction of **9** with ^tBuNC

Treatment of **9** (0.05 g, 0.050 mmol) with ^tBuCN (0.012 g, 0.144 mmol) in CH_2Cl_2 (20 cm^3) followed by chromatography as above gave $[Os_3(CO)_{11}(^tBuNC)]$ (0.040 g, 83%).

3.6. Reaction of **9** with $P(OMe)_3$

A similar reaction of **9** (0.025 g, 0.025 mmol) with $P(OMe)_3$ (0.009 g, 0.073 mmol) followed by a similar work up gave $[Os_3(CO)_{11}\{P(OMe)_3\}]$ (0.021 g, 82%).

3.7. Thermolysis of **9**

An octane solution (40 cm^3) of **9** (0.200 g, 0.200 mmol) was refluxed for 5 h. The solvent was removed under reduced pressure and the residue chromatographed by TLC on silica gel. Elution with hexane–CH_2Cl_2 (10:3, v/v) gave two bands. The first band yielded **7** (0.062 g, 32%) while the second band gave **8** (0.029 g, 15%).

3.8. Reaction of **7** with PPh_3

A similar reaction to that above of **7** (0.110 g, 0.114 mmol) with PPh_3 (0.089 g, 0.339 mmol) in heptane (30 cm^3) at 98°C followed by a similar chromatographic separation gave unconsumed **7** (0.022 g) and $[(\mu\text{-}H)Os_3(CO)_9(\mu\text{-}1,2\text{-}\eta^2\text{-}C_7H_5N_2)(PPh_3)]$ (**12**) (0.065 g, 47%) as yellow micro-crystals from hexane–CH_2Cl_2 at -20°C. (Found: C, 34.12; H, 1.75; N, 2.42. $C_{34}H_{21}N_2O_9Os_3P$ requires: C, 33.94; H, 1.76; N, 2.33). IR (ν(CO), CH_2Cl_2): 2085s, 2044vs, 2014vs, 2000s, 1998m, 1986m, 1965w cm^{-1}; ^1H-NMR ($CDCl_3$): δ 7.71 (dd, 1H, $J = 6.8$, 1.0 Hz), 6.97 (s, 1H), 6.66 (ddd, 1H, $J = 9.3$, 6.8, 1.0 Hz), 6.31 (dq, 2H, $J = 6.8$, 1.0 Hz) -14.71 (d, 1H, $J = 11.8$Hz). $^{31}P\{^1H\}$-NMR ($CDCl_3$): δ 9.5.

3.9. Reaction of **8** with PPh_3

A mixture of **8** (0.150 g, 0.154 mmol) and PPh_3 (0.081 g, 0.309 mmol) in 30 cm^3 of heptane was refluxed for 5 h, the solvent was removed under reduced pressure and the residue chromatographed by TLC on silica gel. Elution with hexane–CH_2Cl_2 (3:1, v/v) gave two bands. The faster moving band gave unconsumed **8** (0.23 g), while the slow band yielded $[(\mu\text{-}H)Os_3(CO)_9(\mu\text{-}1,7\text{-}\eta^2\text{-}C_7H_5N_2)(PPh_3)]$ (**13**) (0.084 g, 45%) as yellow micro-crystals after recrystallization from hexane–CH_2Cl_2 at -20°C. (Found: C, 34.15; H, 1.89; N, 2.45. $C_{34}H_{21}N_2O_9Os_3P$ requires: C, 33.94; H, 1.76; N, 2.33). IR (ν(CO), CH_2Cl_2): 2083s, 2042s, 2006vs, 1993m, 1984m, 1968w cm^{-1}; ^1H-NMR ($CDCl_3$): δ 7.65 (dd, 1H, $J = 6.8$, 1.1 Hz), 7.45 (dd, 1H, $J = 6.8$ and 1.1 Hz), 7.33–7.20 (m, 15H), 6.72 (d, 1H, $J = 1.5$ Hz), 6.54 (d, 1H, $J = 1.5$ Hz), 6.49 (t, 1H, $J = 6.8$ Hz), -13.85 (d, 1H, $J = 15.3$ Hz); $^{31}P\{^1H\}$-NMR ($CDCl_3$): δ 11.4(s).

3.10. Reaction of **8** with imidazo(1,2-a)pyridine

A toluene solution (20 cm^3) of **8** (0.205 g, 0.212 mml) and imidazo(1,2-*a*)pyridine (0.075 g, 0.635 mmol) was refluxed for 5 h. The solvent was removed in vacuo and the residue chromatographed by TLC on silica gel. Elution with hexane–CH_2Cl_2 (3:1, v/v) gave two bands. The faster moving band gave unconsumed **8** (0.050 g), while the slower moving band yielded $[(\mu\text{-}H)_2Os_3(CO)_8(\mu\text{-}1,7\text{-}\eta^2\text{-}C_7H_5N_2)(\mu\text{-}1,2\text{-}\eta^2\text{-}C_7H_5N_2)]$ (**11**) (0.098 g, 45%) as pale yellow crystals from hexane–CH_2Cl_2 at -20°C. (Found: C, 25.69; H, 1.13; N, 5.46. $C_{22}H_{12}N_4O_8Os_3$ requires: C, 25.63; H, 1.17; N, 5.44%). IR (ν(CO), CH_2Cl_2): 2080m, 2047vs, 2027s, 1993vs, 1974m, 1962m cm^{-1}; ^1H-NMR ($CDCl_3$): δ 7.89 (d, 1H, $J = 6.6$ Hz), 7.69 (d, 2H, $J = 6.6$ Hz), 7.30 (d, 2H, $J = 7.3$Hz), 7.21 (d, 1H, $J = 7.3$ Hz), 7.19 (d, 1H, $J = 6.3$ Hz), 7.01 (s, 1H), 6.59 (overlapping d, 2H, $J = 6.5$ Hz), -11.49 (s, 1H), -13.66 (s, 1H).

3.11. Reaction of **7** with imidazo(1,2-a)pyridine

A similar reaction to that above of **7** (0.155 g, 0.166 mmol) and imidazo(1,2-*a*)pyridine (0.059 g, 0.498 mmol) in refluxing toluene (15 cm^3) for 5 h followed by chromatographic separation yielded unreacted **7** (0.015 g) and $[(\mu\text{-}H)_2Os_3(CO)_8(\mu\text{-}1,2\text{-}\eta^2\text{-}C_7H_5N_2)_2]$ (**10**) (0.056 g, 34%) after recrystallization from hexane–CH_2Cl_2 at -20°C. (Found: C, 2.92; H, 1.45; N, 5.52. $C_{22}H_{12}N_4O_8Os_3$ requires: C, 25.63; H, 1.17; N, 5.44%). IR (ν(CO), CH_2Cl_2): 2078m, 2045vs, 2027s, 1990vs, 1971m, 1960m cm^{-1}; ^1H-NMR ($CDCl_3$): δ 7.95 (d, 1H, $J = 6.8$ Hz), 7.78 (m, 3H) 7.57 (m, 2H), 7.15 (s, 1H), 7.07 (s, 1H), 6.68 (m, 2H), -11.66 (s, 1H), -13.18 (s, 1H).

3.12. X-ray crystallography

Crystallographic measurements for **7**, **8**, **9** and **11** were made on a Delft Instruments FAST TV area detector diffractometer positioned at the window of a

Table 5
Crystal data and details of data collection and structure refinement for [(μ-H)Os$_3$(CO)$_{10}$(μ-1,2-η^2-C$_7$H$_5$N$_2$)] (**7**), [(μ-H)Os$_3$(CO)$_{10}$(μ-1,7-η^2-C$_7$H$_5$N$_2$)] (**8**), [Os$_3$(CO)$_{11}$(η^1-C$_7$H$_6$N$_2$)] (**9**) and [(μ-H)$_2$Os$_3$(CO)$_8$(μ-1,7-η^2-C$_7$H$_5$N$_2$)(μ-1,2-η^2-C$_7$H$_5$N$_2$] (**11**) [a]

	Compound **7**	Compound **8**	Compound **9**	Compound **11**
Chemical formula	$C_{17}H_6N_2O_{10}Os_3$	$C_{17}H_6N_2O_{10}Os_3$	$C_{18}H_6N_2O_{11}Os_3$	$C_{22}H_{12}N_4O_8Os_3$
Formula weight	968.84	968.84	996.85	1030.96
Crystal system	Monoclinic	Monoclinic	Triclinic	Monoclinic
Space group	$P2_1/c$ (no. 14)	$C2/c$ (no. 15)	$P\bar{1}$ (no. 2)	$P2_1/c$ (no. 14)
a (Å)	9.507(2)	30.836(7)	8.974(2)	16.672(5)
b (Å)	12.322(3)	7.6749(9)	10.011(2)	9.093(3)
c (Å)	18.653(3)	17.428(3)	12.665(3)	16.766(6)
α (°)	90	90	101.97(2)	90
β (°)	103.278(2)	95.33(2)	94.07(2)	101.24(2)
γ (°)	90	90	100.91(2)	90
V (Å^3)	2126.8(8)	4106.6(13)	1085.7(4)	2493.0(14)
Z	4	8	2	4
Crystal size (mm)	$0.18 \times 0.15 \times 0.10$	$0.22 \times 0.16 \times 0.14$	$0.22 \times 0.16 \times 0.10$	$0.30 \times 0.15 \times 0.08$
D_c (g cm^{-3})	3.026	3.134	3.049	2.747
μ(Mo–K$_\alpha$) (cm^{-1})	179.36	185.78	175.75	153.07
Absorption correction factors	0.823–1.149	0.779–1.173	0.792–1.021	0.766–1.242
θ range for data collection (°)	2.00–24.99	2.35–24.97	2.13–24.88	2.48–25.08
Index ranges	$-8 \le h \le 11$	$-34 \le h \le 33$	$-9 \le h \le 10$	$-17 \le h \le 18$
	$-14 \le k \le 13$	$-8 \le k \le 8$	$-11 \le k \le 11$	$-10 \le k \le 8$
	$-21 \le l \le 21$	$-20 \le l \le 16$	$-9 \le l \le 14$	$-19 \le l \le 19$
Reflections collected	8299	8437	4761	9565
Unique reflections	3225	3182	3061	3744
R_{int}	0.0785	0.0794	0.0815	0.0809
Goodness-of-fit on F^2	0.805	0.887	1.169	0.898
Data/parameters in the refinement	3225/289	3440/289	3061/307	3744/334
Final R [b] indices	$R_1 = 0.0617$ (0.0361)	$R_1 = 0.0475$ (0.0351)	$R_1 = 0.0696$ (0.0664)	$R_1 = 0.0685$ (0.0418)
	$wR_2 = 0.0730$ (0.0.0693)	$wR_2 = 0.0735$ (0.0713)	$wR_2 = 0.1707$ (0.1687)	$wR_2 = 0.0836$ (0.0803)
Largest difference peak and hole (e Å^{-3})	2.068 and −2.012	2.903 and −2.013	1.560 and −1.441	1.792 and −1.386

[a] Details in common: FAST area detector diffractometer; $\lambda = 0.71069$ Å; $T = 150$ K; crystal colour: yellow; refinement method: full-matrix least-squares on F^2.

[b] $R_1 = \Sigma(F_o - F_c)/\Sigma(F_o)$; $wR_2 = [\Sigma\{w(F_o^2 - F_c^2)^2\}/\Sigma\{w(F_o^2)^2\}]^{1/2}$; $w = 1/[\sigma^2(F_o^2) + (aP)^2]$, where $P = [(F_o^2) + 2F_c^2]/3$ with $a = 0.0114$ (**7**), 0.0181 (**8**), 0.1184 (**9**) and 0.0202 (**11**). R-values calculated for data with $I > 2\sigma(I)$ are given in parentheses.

rotating anode generator, using Mo–K$_\alpha$ radiation ($\lambda = 0.71069$ Å) in a manner described previously [37]. In all cases the unit cell parameters were obtained by least-squares refinement of the diffractometer angles for 250 reflections. All data sets were corrected for absorption using DIFFABS [38]. The structures were solved by direct methods (SHELXS-86) [39], developed via difference syntheses, and refined on F^2 by full-matrix least-squares (SHELXL-93) [40] using all unique data with intensities greater than 0. The non-H atoms were treated anisotropically, but it was necessary to refine the C(2) and C(6) atoms in **7**, and C(1), C(4), C(7), C(8) and C(16) atoms in **8** with ISOR constraints of 0.002 and 0.007, respectively. The bridging hydrides were experimentally located but not refined. The ring hydrogen atoms were included in calculated positions (riding model). Crystallographic data and the refinement details together with the final R-values are presented in Table 5.

4. Supplementary material

Crystallographic data for the structural analyses have been deposited with the Cambridge Crystallographic Data Centre, CCDC nos. 118278 (**7**), 118277 (**8**), 118279 (**9**) and 118280 (**11**). Copies of this information may be obtained free of charge from The Director, CCDC, 12 Union Road, Cambridge CB2 1EZ, UK (Fax: +44-1222-336-0333) or e-mail: deposit@ccdc.cam.ac.uk or http://www.ccdc.cam.ac.uk).

Acknowledgements

This work was supported by the Fonds der Chemischen Industrie and by the Commission for the European Communities. S.E.K. acknowledges the Alexander von Humboldt Foundation for a fellowship. M.B.H. and K.M.A.M. acknowledge the EPSRC support of the X-ray crystallography facilities at

Cardiff. E.R. thanks the National Science Foundation (CHE 9625367) for support.

References

[1] A. Eisenstadt, C.M. Giandomenico, M.F. Frederick, R.M. Laine, Organometallics 4 (1985) 2033.

[2] R.H. Fish, T. Kim, J.L. Stewart, J.H. Bushweller, R.K. Rosen, J.W. Dupon, Organometallics 5 (1986) 2193.

[3] R.H. Fish, E. Baralt, H.S. Kim, Organometallics 10 (1991) 1965.

[4] R.H. Fish, H. Kim, R.H. Fong, Organometallics 10 (1991) 770.

[5] R.H. Fish, E. Baralt, S.J. Smith, Organometallics 10 (1991) 54.

[6] E. Baralt, S.J. Smith, J. Hurwitz, I.T. Horvath, R.H. Fish, J. Am. Chem. Soc. 114 (1992) 5187.

[7] R.H. Fish, in: R. Ugo (Ed.), Aspects of Homogeneous Catalysis, Kluwer, Dordrecht, The Netherlands, 1990, pp. 65–83.

[8] E. Rosenberg, S.E. Kabir, K.I. Hardcastle, M. Day, E. Wolf, Organometallics 9 (1990) 2214 and references therein.

[9] S.E. Kabir, M. Day, M. Irving, T. McPhillips, H. Minassian, E. Rosenberg, K.I. Hardcastle, Organometallics 10 (1991) 3997.

[10] M. Day, S. Hajela, S.E. Kabir, M. Irving, T. McPhillips, E. Wolf, K.I. Hardcastle, E. Rosenberg, L. Milone, R. Gobetto, D. Osella, Organometallics 10 (1991) 2743.

[11] M.P. Cifuentes, M.G. Humphrey, B.W. Skelton, A.H. White, J. Organomet. Chem. 458 (1993) 211.

[12] S.E. Kabir, E. Rosenberg, M. Day, K.I. Hardcastle, M. Irving, J. Clust. Sci. 5 (1994) 481.

[13] J.A. Cabeza, L. Landazuri, L.A. Oro, A. Tiripicchio, M. Tiripicchio, J. Organomet. Chem. 322 (1987) C11.

[14] J.A. Cabeza, L.A. Oro, A. Tiripicchio, M. Tiripicchio Camellini, J. Chem. Soc. Dalton Trans. (1988) 1437.

[15] M.A. Pellinghelli, J.A. Cabeza, L.A. Oro, Tiripicchio, J. Chem. Soc. Dalton Trans. (1990) 1509.

[16] G. Süss-Fink, T. Jenke, H. Heitz, M.A. Pellighellia, A. Tiripicchio, J. Organomet. Chem. 379 (1989) 311.

[17] G.A. Foulds, B.F.G. Johnson, J. Lewis, J. Organomet. Chem. 294 (1985) 123.

[18] S. Aime, R. Gobetto, F. Padovan, M. Botta, E. Rosenberg, R. Gellert, Organometallics 6 (1987) 2074.

[19] M.W. Day, S. Haiela, K.I. Hardcastle, E. Rosenberg, R. Gobelto, L. Milone, D. Osella, R. Gellert, Organometallics 9 (1990) 913.

[20] K.I. Hardcastle, H. Minassian, A.J. Arce, Y. De Sanctis, A.J. Deeming, J. Organomet. Chem. 368 (1989) 119.

[21] R. Agarwala, K.A. Azam, R. Dilshad, S.E. Kabir, R. Miah, M. Shahiduzzaman, M.B. Hursthouse, K.M.A. Malik, J. Organomet. Chem. 492 (1995) 135.

[22] K.A. Azam, M.B. Hursthouse, S.A. Hussain, S.E. Kabir, K.M.A. Malik, M.M. Rahman, E. Rosenberg, J. Organomet. Chem. 559 (1998) 81.

[23] K.A. Azam, M.B. Hursthouse, S.E. Kabir, K.M.A. Malik, H. Vahrenkamp, Inorg. Chem. Commun. 1 (1998) 402.

[24] K.A. Azam, R. Dilshad, S.E. Kabir, K. Khatoon, L. Nessa, M.M. Rahman, E. Rosenberg, M.B. Hursthouse, K.M.A. Malik, A.J. Deeming, J. Chem. Soc. Dalton Trans. (1996) 1731.

[25] S.E. Kabir, D.S. Kowaite, E. Rosenberg, K.I. Hardcastle, W. Cresswell, J. Grindstaff, Organometallics 14 (1995) 3611.

[26] M.R. Churchill, B.G. DeBoer, Inorg. Chem. 16 (1977) 878.

[27] S.E. Kabir, T.A. Siddiquee, E. Rosenberg, R. Smith, M.B. Hursthouse, K.M.A. Malik, K.I. Hardcastle, M. Visi, J. Clust. Sci. 9 (1998) 185.

[28] B.F.G. Johnson, J. Lewis, D.A. Pippard, J. Chem. Soc. Dalton Trans. (1981) 407.

[29] P.A. Dawson, B.F.G. Johnson, J. Lewis, J. Puga, P.R. Raithby, J. Rosales, J. Chem. Soc. Dalton Trans. (1982) 235.

[30] B.F.G. Johnson, J. Lewis, W.J.H. Nelson, M.A. Pearsall, P.R. Raithby, M.J. Rosales, M. McPartlin, A. Sironi, J. Chem. Soc. Dalton Trans. (1987) 327.

[31] K.A. Azam, R. Dilshad, S.E. Kabir, R. Miah, M. Shahiduzzaman, E. Rosenberg, K.I. Hardcstle, M.B. Hursthouse, K.M.A. Malik, J. Clust. Sci. 7 (1996) 49.

[32] S.M.T. Abedin, K.A. Azam, M.B. Hursthouse, S.E. Kabir, K.M.A. Malik, R. Miah, H. Vahrenkamp, J. Organomet. Chem. 564 (1998) 133.

[33] M.G. Humphery, B.W. Skelton, A.H. White, J. Organomet. Chem. 513 (1996) 201.

[34] S.E. Kabir, E. Rosenberg, M. Day, K.I. Hardcastle, E. Wolf, T. McPhillips, Organometallics 14 (1995) 721.

[35] C.C. Yin, A.J. Deeming, J. Chem. Soc. Dalton Trans. (1975) 2091.

[36] M. Day, D. Espitia, K.I. Hardcastle, S.E. Kabir, E. Rosenberg, R. Gobetto, L. Milone, D. Osella, Organometallics 10 (1991) 3550.

[37] J.A. Darr, S.R. Drake, M.B. Hursthouse, K.M.A. Malik, Inorg. Chem. 32 (1993) 5704.

[38] N.P.C. Walker, D. Stuart, Acta Crystallogr. Sect. A 39 (1983) 158.

[39] G.M. Sheldrick, Acta Crystallogr. Sect. A 46 (1990) 467.

[40] G.M. Sheldrick, SHELXL-93 program for crystal structure refinement, University of Göttingen, Germany, 1993.